

High precision dual-inlet IRMS measurements of the stable isotopes of CO₂ and the N₂O/CO₂ ratio from polar ice core samples

T. K. Bauska¹, E.J. Brook¹, A.C. Mix¹, A. Ross¹

[1] College of Earth, Ocean and Atmospheric Sciences, Oregon State University, Corvallis, OR 97331, USA

Correspondence to: T. K. Bauska (bauskat@geo.oregonstate.edu)

Abstract

An important constraint on mechanisms of past carbon cycle variability is provided by the stable isotopic composition of carbon in atmospheric carbon dioxide ($\delta^{13}\text{C-CO}_2$) trapped in polar ice cores, but obtaining very precise measurements has proven to be a significant analytical challenge. Here we describe a new technique to determine the $\delta^{13}\text{C}$ of CO₂ at exceptional precision, as well as measuring the CO₂ and N₂O mixing ratios. In this method, ancient air is extracted from relatively large ice samples (~400 grams) with a dry-extraction "ice-grater" device. The liberated air is cryogenically purified to a CO₂ and N₂O mixture and analyzed with a micro-volume equipped dual-inlet IRMS (Thermo MAT 253). The reproducibility of the method, based on replicate analysis of ice core samples, is 0.02‰ for $\delta^{13}\text{C-CO}_2$ and 2 ppm and 4 ppb for the CO₂ and N₂O mixing ratios, respectively (1-sigma pooled standard deviation). Our experiments show that minimizing water vapor pressure in the extraction vessel by housing the grating apparatus in a ultra-low temperature freezer (-60°C) improves the precision and decreases the experimental blank of the method. We describe techniques for accurate calibration of small samples and the application of a mass spectrometric method based on source fragmentation for reconstructing the N₂O history of the atmosphere. The oxygen isotopic composition of CO₂ is also investigated, confirming previous observations of oxygen exchange between gaseous CO₂ and solid H₂O within the ice archive. These data offer a possible constraint

1 on oxygen isotopic fractionation during H₂O and CO₂ exchange below the H₂O bulk
2 melting temperature.

3

4 **1 Introduction**

5 The air occluded in polar ice is an outstanding archive of the ancient atmosphere. Over
6 the past few decades, highly specialized analytical methods have yielded excellent
7 records of climate and biogeochemical processes. Measuring trace gases from ice core
8 samples presents a number of significant technical challenges, most notably how to
9 extract the air from the ice without significantly altering the in situ composition, and how
10 to make accurate and precise measurements on limited amounts of air. Many current ice
11 core δ¹³C-CO₂ methods have precision of about 0.1‰ (see below). This limits
12 interpretation of mechanisms because the uncertainty is about 1/3 of the full dynamic
13 range observed on glacial-interglacial timescales (~0.3‰) (Schmitt et al., 2012).
14 Additionally, fluxes of carbon depleted in ¹³C from the terrestrial biosphere (~-25‰) on
15 decadal to centennial timescales leave an isotopic imprint on the atmosphere (~-6.5‰) of
16 about -0.03‰ per ppm CO₂ (see below) (Trudinger et al.,
17 2002). With modern atmospheric measurements capable of precision of 0.01‰ (Masarie
18 et al., 2001), improvements in ice core methods have huge potential to constrain paleo-
19 atmospheric isotopic budgets and the mechanisms of CO₂ variability.

20 Early efforts to analyze carbon isotope ratios of CO₂ in ice cores using milling devices on
21 large samples with dual-inlet IRMS measurements obtained precisions of about 0.1‰
22 (Friedli and Stauffer, 1986; Leuenberger et al., 1992). Subsequently, dual-inlet IRMS
23 measurements improved the constraints on the Last Glacial termination and Holocene
24 history (Indermuhle et al., 1999; Smith et al., 1999) but precision remained about 0.08‰.
25 More recently, gas-chromatographic IRMS (GC-IRMS) methods have significantly
26 decreased the required sample size, which allows for greater sampling resolution and
27 simpler mechanical crushers. However, precision with these techniques is still about
28 0.1‰ (Elsig et al., 2009; Leuenberger et al., 2003; Lourantou et al., 2010; Schaefer et al.,
29 2011). A novel method that employs sublimation to release the occluded air followed by
30 GC-IRMS measurement techniques has made significant improvement to the precision

1 obtained from small samples (0.05-0.09‰) (Schmitt et al., 2011). The highest precision
2 measurements (0.025-0.05‰) to date were obtained from the Law Dome ice core
3 spanning the last millennium using an large volume ice grater and dual-inlet technique
4 (Francey et al., 1999). However, this record was recently augmented and revised to
5 account for a significant shift in the mean values of many of the measurements. When an
6 estimate of changing accuracy was included, the average uncertainty for individual
7 measurements was similar to that of other methods, about 0.06‰ (Rubino et al., 2013).

8
9 Due to the limited availability of ice samples, many methods are designed to minimize
10 sample consumption at the expense of precision for an individual measurement.
11 Sometimes this lower precision can be balanced by ability to collect larger numbers of
12 replicates quickly, or to pursue higher-resolution sampling schemes. GC-IRMS
13 techniques that require very small samples have come to dominate ice core $\delta^{13}\text{C-CO}_2$
14 measurements. We approach the problem from a different perspective and aim to
15 increase the precision of the measurement with larger samples such that fewer
16 measurements are required to extract a low-noise signal from the ice core.

17
18 While dual-inlet IRMS typically offers better precision than GC-IRMS, it also presents
19 two distinct problems that we address here. Firstly, N_2O interferes isobarically with CO_2 .
20 Ice core N_2O is generally atmospheric in origin, but it is occasionally produced *in situ* in
21 large amounts possibly by microbial degradation of organic matter (Miteva et al., 2007).
22 With changes in the N_2O -to- CO_2 ratio up to 30% over a glacial- interglacial cycle, the
23 magnitude of the $\delta^{13}\text{C-CO}_2$ correction can range from about 0.2-0.3‰, introducing a
24 systematic error. N_2O can be readily separated from CO_2 by a GC, but is practically
25 impossible to separate from CO_2 cryogenically or in a chemically destructive manner
26 without altering the isotopic composition of the CO_2 . Dual-inlet mass spectrometry
27 measurements thus require an accurate estimate of the N_2O -to- CO_2 ratio in the ion beam.
28 Previous methods derived the N_2O -to- CO_2 ratio include: a low precision mass
29 spectrometer method that was susceptible to experimental *in situ* N_2O production in the
30 extraction apparatus (Friedli and Siegenthaler, 1988), offline measurements on an aliquot
31 of the same sample air (Francey et al., 1999), or from an interpolation of separate data

1 sets to the depths of the samples used for isotopic measurements (Smith et al., 1999). We
2 utilize a method that measures the $^{14}\text{N}^{16}\text{O}$ fragment produced in the mass spectrometer
3 source to determine the abundance and ionization efficiency of N_2O (Assonov and
4 Brenninkmeijer, 2006). We demonstrate that the method is very precise for estimating
5 the interference correction and provides, as a byproduct, a robust record of the ice core
6 N_2O history.

7

8 Secondly, contamination from hydrocarbon-rich drilling fluid is minimized by GC
9 cleanup in GC-IRMS methods but could cause major problems for dual-inlet
10 measurement if the catenated molecules, highly susceptible to fragmentation, reach the
11 ion source. We observe that drilling fluid contamination can be effectively monitored
12 using higher-mass detectors of high sensitivity. Along with additional cleaning steps
13 (described below), this completely mitigates the problem in high-quality ice.

14

15 **2 Ice Archives**

16 Three ice archives were utilized in this study (Table 1). The Taylor Glacier archive is a
17 “horizontal” ice core from an ablating section of ice on the Taylor Glacier, McMurdo Dry
18 Valleys, Antarctica (77.75 °S, 161.75 °E). The section encompasses a complete
19 stratigraphic section of the last deglaciation from about 20,000 to 10,000 years before
20 present. WDC05A is a relatively shallow depth (~300 m) core from the West Antarctic
21 Ice Sheet (WAIS) Divide Ice Core Site (79.467 °S, 112.085 °W) and spans the last 1000
22 years (Mitchell et al., 2011). WDC06A is the main deep core from WAIS Divide and the
23 data presented here span an interval from about 250-350 m (1250-750 yr B.P.).

24

25 **3 Experimental Procedure**

26 **3.1 Ice Grater Apparatus Design**

27 The ice grater extraction vessels are constructed from a stainless steel, electropolished
28 cylinder, 25 cm in length, and capped on both ends with copper gasket sealed, 6-3/4 inch
29 CF Flanges (Kurt Lesker Company). The flanges have been machined to remove excess
30 weight from the exterior and bored to allow for a 3/8 inch outlet. The interior of the ice

1 grater contains a perforated stainless steel sheet, molded to form a semi-cylinder, and
2 attached to the interior walls of the ice grater with spot welds. The perforations resemble
3 the abrasive surface one finds on a household cheese grater used to finely grate a hard
4 cheese.

5
6 Most of the components on the extraction line are stainless steel and are joined with
7 either tungsten inert gas welds or copper gasket-sealed fittings (Swagelok VCR). The
8 combination of both welds and gasket fittings lowers the chance of leaks but also
9 maintains modularity. All the valves are bellows-sealed with spherical metal stem-tips
10 (majority are Swagelok BG series). The pumping system is comprised of a turbo-
11 molecular pump (Alcatel Adixen ATP 80) and scroll pump (Edwards XDS5).

12
13 During air extraction, the ice grater chamber is housed in an ultra-low temperature freezer
14 at -60°C (So-low, Inc.) with custom-built feed-through ports. The grater rests on an
15 aluminum frame fixed to a linear slide apparatus, which is driven by a pneumatic piston
16 (SG Series; PHD, Inc). A system of pneumatic valves allows the operator to control the
17 stroke length and frequency of the motion. The pneumatic piston sits outside the freezer
18 and the ice grater cradle slides on steel rods with teflon coated bushings. The
19 combination of keeping the greased pneumatic piston outside of the freezer and replacing
20 the standard lubricated ball bearings with teflon bushings proved effective in keeping the
21 moving parts of the ice grater shaker from seizing up in the cold.

22 23 **3.2 Air Extraction**

24 About 14 hours prior to the first analysis, ice samples stored in a -25°C freezer are cut
25 and shaped with a bandsaw. The dimensions of the cut sample are typically 5 x 6 x 15
26 cm with masses ranging between 400 to 550 grams depending on sample availability.
27 Roughly 1-3 mm of ice from the cut surface of the sample is removed with a ceramic
28 knife as a precautionary cleaning step.


29
30 Ice samples from coring campaigns that did not use drill fluid (WDC05A and Taylor
31 Glacier in this study) required very minor cleaning. However, samples exposed to



1 drilling fluid composed of **HCFC-141B** and Isopar-K (WDC06A in this study) required
2 an extensive cleaning procedure involving removal of about a 1 cm thickness from the
3 exterior of the ice core piece to avoid potential micro-fractures filled with drill fluid.

4
5 After cleaning, two samples are each loaded and sealed in their respective ice grater. The
6 graters are placed into the -60°C freezer, attached to the extraction line (Figure 1) via an
7 opening in the freezer wall, and pumped to vacuum at about 0.02 Torr (in the presence of
8 water vapor) for about 30 minutes. The ice graters are detached from the vacuum line,
9 but remain sealed under vacuum in the freezer for a period of about 12 hours. It is
10 important to let the ice completely cool down because it minimizes the amount of water
11 vapor in the extraction vessel during grating.

12
13 Prior to the sample analysis at least three aliquots of NOAA reference standard air are
14 processed and measured like a sample, with the exception of exposure to the ice grater
15 portion of the system (see description of air extraction below). After the initial standard
16 runs are completed, the first chilled ice grater is reattached to the vacuum line, checked to
17 make sure no significant leaks developed during storage, and pumped for an additional 45
18 minutes. The ice grater is then detached and placed on the pneumatic slide.

19
20 To grate the ice, the pneumatic piston drives the ice grater horizontally with a translation
21 of 20 cm at around 2 Hz for 30 minutes. This is sufficient to grate about 75% of the ice
22 into <1 cm diameter fragments. Typically, an ellipsoid shaped piece of about 100 grams
23 remains intact, which can be used at a later date for additional analysis. Based on
24 manometric measurements of the air extracted from a bubble ice sample, and typical total
25 air content for ice (0.1 cubic centimeter per gram), the overall air extraction efficiency
26 averages about 60%. **This is on the low end of typical dry extraction methods**  an area
27 for future improvement. Our experiments with fully and partially clathrated ice showed
28 marked decreases in the grating efficiency (that is, the ice was still grated finely, but the
29 piece remaining intact after a long period of time was very large), and the measurements
30 in this type of ice were deemed too impractical for now.

31

1 After grating, the ice grater is re-coupled to the extraction line (Figure 1). At this point,
2 the ice grater contains about 5 Torr of sample air. A small aliquot of the sample, <1 cc, is
3 isolated from the ice grater in the extraction line (volume between Valves 1 and 15). The
4 air sample is cyropumped through a coiled, stainless steel trap held at 170 K (with liquid
5 nitrogen cooled ethanol) to remove water vapor and condensed at 11 K in a 7 cc sample
6 tube held in a closed-cycle cryocooler (10K-CCR, Janis Research Company). This air
7 sample is warmed to room temperature and stored for a few hours before being analyzed
8 with an Agilent 7890A GC to determine the CO₂ mixing ratio. The CO₂ measurement is
9 similar to previous methodology at Oregon State University (*Ahn et al., 2009*), whereby
10 CO₂ is separated with a Porapak Q 80/100 mesh column, reduced to CH₄ with a nickel
11 catalyst, and measured with a flame ionization detector (FID). However, whereas the
12 previous method uses a manometer in the sample loop to determine the total air injected
13 into the GC, we employ a thermal conductivity detector (TCD) to measure amount of O₂
14 and N₂ in the sample. This design minimizes the volume required for sample injection.
15 Standard gases calibrated by NOAA on 2007 WMO Mole Fraction Scale are used to
16 reference the sample mixing ratio (Table 2) (Zhao et al., 1997).

17
18 To extract the CO₂ and N₂O from the remaining air sample, the "w" shaped stainless steel
19 trap is cooled with liquid nitrogen to 80 K (Figure 1, between valves 10 and 12). Any
20 residual non-condensable gases in the the sample air is passed over the coiled water trap
21 (~170 K) and the "w" CO₂-N₂O trap (~80 K) by pulling the air from the ice grater
22 through the extraction line with a turbo-molecular pump. The flow is regulated using a
23 spherical stem-tip valve to remain less than 5 cm³ per minute, to maximize the
24 probability that CO₂ and N₂O are trapped as the non-condensable gases are pumped
25 away. After about 5 minutes of regulating the flow with about 80% of the air extracted,
26 the valve is fully opened and sample extraction continues for an additional 15 minutes
27 until about 99% of the non-condensable gas has been removed (air pressure remaining
28 about 0.05 Torr). The "w" shaped trap, with the liquid nitrogen only submerging the
29 lower portion of the trap, effectively has two closely spaced "u" traps. This proved to be
30 important for preventing the loss of CO₂ in the fast moving stream of air (for example by
31 advecting flakes of frozen CO₂), without greatly decreasing the conductance of the

1 vacuum line. Though the cryocooler also showed promise as a residual air pump and the
2 turbo-molecular pumping system ultimately proved more efficient at extracting the last
3 few percent of sample without any significant isotopic fractionation.

4
5 With the CO₂ and N₂O held in the "w" trap, valves 7 and 12 are closed (Figure 1) to
6 isolate the sample from the portion of the extraction line exposed to water vapor. The
7 "w" trap is warmed to 170 K by replacing the liquid nitrogen Dewar flask with a chilled
8 ethanol-slush Dewar flask. This releases the CO₂ and N₂O but secures any water that
9 may have passed through the primary water trap. The amount of CO₂ and N₂O is then is
10 determined manometrically (MKS Baratron). The sample amount is used to predict the
11 subsequent sample inlet pressure on the dual-inlet and pre-adjust the reference bellows
12 accordingly. To transfer the now dry CO₂ and N₂O to the dual-inlet system, a small
13 stainless steel tube attached to the line with a VCR fitted valve is immersed in liquid
14 nitrogen for about 1 minute, allowing the gases to condense in the tube. This tube is
15 removed from the extraction line and attached to the sample side of the dual-inlet prior to
16 analysis with a VCR copper sealed gasket.

18 3.3 Dual-Inlet IRMS Measurement

19 The dual-inlet portion of the analysis is a computer controlled routine (Thermo Fisher
20 Scientific, Inc.), modified slightly to accommodate the small samples and the
21 measurement of the m/z 30 beam. The CO₂ and N₂O bypass the sample bellow and are
22 condensed in a 150 µl cold finger known as the "micro-volume" for a period of 120
23 seconds. Valves are closed so that the microvolume bleeds only to the changeover valve
24 via a crimped capillary. The microvolume is warmed to 28 °C to allow the CO₂ and N₂O
25 to leak into the ion source.

26
27 With the reference side pre-adjusted to the expected sample size, the automated bellow
28 adjustment period is typically minimal. Once the reference beam is within about 100 mV
29 of the sample intensity, typically by the time the sample beam intensity is about 3000
30 mV, the reference side micro-volume (also 150 µl) is isolated from its bellow, and the
31 dual-inlet measurement begins.

1
2 The operating range for the dual-inlet pressure was between about 0.01-0.015 bar,
3 equivalent to about a sample size of 1.5-2.25 bar $\mu\text{L CO}_2$. The measurement is comprised
4 of eight dual-inlet cycles, each with an integration time of 8 seconds and idle time for
5 changeover switching of 15 seconds. By the end of the measurement, the sample beam is
6 typically 1000-2000 mV. A careful balance of the reference and sample capillary crimps
7 and pre-adjustment of the reference bellows was required to keep the difference in m/z 44
8 beam intensity between the reference and sample beam both small and consistent (mean
9 offset = 77 mV, 1-sigma standard deviation = 40 mV). After the CO_2 analysis is
10 complete, the instrument jumps the major ion beam to m/z 30 and measures this intensity
11 on the sample and reference beams. The ^{17}O abundance correction follows the
12 formulation of Santrock et al., 1985. All traps are heated to about 50 °C and pumped
13 before the start of the next analysis.
14

15 **3.4 Calibration**

16 In order to calibrate the isotopic values of the sample measurements, a working reference
17 gas of pure CO_2 (Oztech) was measured on a daily basis against at least six aliquots of a
18 NOAA standard air (hereafter: NOAA1). The “NOAA” standards were calibrated by the
19 INSTAAR Stable Isotope Lab, University of Colorado to the VPDB- CO_2 scale with the
20 primary reference as NBS-19 (isotopic values of all standards are in Table 2). The
21 NOAA standard gas aliquots were processed with the sample extraction line both before
22 and after the samples were analyzed. Typically, the mean of all six NOAA standard gas
23 measurements was used as one-point calibration for the working reference gas. All the
24 standard gas measurements, relative to a fixed working reference gas value are shown in
25 Figure 2.

26
27 Over the analysis period, the 1-sigma standard deviation of the NOAA1 standard was
28 0.03 and 0.13‰, for $\delta^{13}\text{C}$ and $\delta^{18}\text{O}$ respectively. However, the signal is not completely
29 random, the $\delta^{13}\text{C}$ and $\delta^{18}\text{O}$ co-vary on the time frame of a few days ($R^2 = 0.13$; slope =
30 1.78; intercept = 7.42). Often, the standard gas appears to become more
31 depleted, or alternatively, the working reference gas become more enriched, by about

1 0.075‰ in $\delta^{13}\text{C}$ over the course of a few days, with the trend reversed when the working
2 reference gas is replenished. This trend was confirmed during early experimentation and
3 sample analysis by occasionally measuring the reference bellow against the same gas in
4 the sample bellow that was only lightly consumed of the course of analysis. Assuming
5 no leaks were present, this suggests that the gas in the reference bellows was becoming
6 more enriched if not replenished frequently.

7
8 Reference gas enrichment over time may be at least partially due to a mass dependent
9 distillation process operating as the gas in reference bellow is consumed. Because the
10 amount of gas in the bellows has to be very small to accommodate the lower sample size
11 (e.g. 10 mbar at 100% expansion \approx 0.25 mbar mL), the gas is quickly consumed over a
12 few days of analysis, typically 10% per day. Given Rayleigh distillation, this would
13 roughly correspond to a fractionation factor of about 1‰ for $\delta^{13}\text{C}$ and 2‰ for $\delta^{18}\text{O}$.
14 While much smaller than the expected $\delta^{13}\text{C}$ fractionation if molecular flow dominated the
15 flow-regime (\sim 11‰) (Halsted and Nier, 1950), it does suggests the flow is not
16 completely viscous at all times. Ultimately, the effect on precision of the sample
17 measurements is negligible because the working reference gas is calibrated to the NOAA
18 standard every day. From a practical standpoint, it requires that the working reference
19 gas is replenished about every other day and gas consumption is minimized.

20
21 Additional experiments with a second NOAA standard (NOAA2) of similar $\delta^{13}\text{C}$ -CO₂ (-
22 8.106‰) but very different $\delta^{18}\text{O}$ -CO₂ (-0.777‰), CO₂ (\sim 150 ppm) and N₂O (\sim 321 ppb),
23 as well as another working reference gas with very different $\delta^{13}\text{C}$ (-3.58‰) were made to
24 test the validity of a one-point calibration (see Table 2). The accuracy of the NOAA
25 calibration scale was also checked by measuring the working reference gases against the
26 carbonate standard NBS-19 with a Kiel Device, allowing for an independent in-house
27 calibration of the NOAA standards (reported in Table 2). With the NOAA1 standard
28 being measured over 400 times against the working reference, the INSTAAR-SIL and in-
29 house calibration converge within 0.001‰ for $\delta^{13}\text{C}$ -CO₂. The difference between the
30 calibrations for the NOAA2 standard $\delta^{13}\text{C}$ -CO₂ (0.034‰) is probably a product of the

1 significantly less frequent measurement of the NOAA2 standard, which was used almost
2 exclusively to calibrate the N₂O measurement.

3

4 **3.5 N₂O Measurement**

5 To correct the IRMS measurements for the isobaric interference of N₂O, we employ a
6 method that uses the fragmentation of N₂O in the source to estimate both the N₂O-to-CO₂
7 ratio and the ionization efficiency of N₂O (Assonov and Brenninkmeijer, 2006). The ion
8 beam at m/z 30 is composed primarily of ¹⁴N¹⁶O⁺ derived from N₂O and ¹²C¹⁸O⁺ derived
9 from CO₂, is compared to the m/z 44 intensity in both the sample (a unknown mixture of
10 N₂O and CO₂) and the reference (pure CO₂). The difference between m/z 30 signal of the
11 sample and the reference is a measure of the N₂O in sample that is has been ionized in the
12 source. The fragmentation yield of ¹⁴N¹⁶O⁺ from N₂O (³⁰Intensity/⁴⁴Intensity of N₂O =
13 ³⁰R-N₂O) and the ionization efficiency of N₂O (E-N₂O) must be determined in order to
14 completely estimate the N₂O-to-CO₂ ratio. This technique differs from a previous method
15 applied to ice core air which used the m/z 30-to-28 ratio (Friedli and Siegenthaler, 1988)
16 which can be susceptible m/z 28 contamination by ¹⁴N¹⁴N⁺ from small leaks (Assonov
17 and Brenninkmeijer, 2006).

18

19 Idealized experiments with pure N₂O and/or N₂O diluted in an inert gas can be performed
20 to quantify these parameters. We calibrated the method using two NOAA calibrated
21 standards with very different N₂O-to-CO₂ ratios (0.00091 and 0.00214) to estimate the
22 two unknowns. Our initial calibration found effective values of ³⁰R-N₂O = 0.19 and E-
23 N₂O = 0.70.

24

25 We report N₂O in terms of ppb, rather than the more cumbersome N₂O-to-CO₂ ratio that
26 is directly measured. To calculate the N₂O and associated errors of the NOAA standard
27 measurements in terms of ppb we use a constant CO₂ concentration known from the
28 NOAA calibration. For the samples, we use the CO₂ concentration measured on our GC
29 system, introducing a source of error from the offline analysis.

30

1 Because only the NOAA1 standard was analyzed on a day-to-day basis, only one single
2 N₂O-to-CO₂ ratio was used to monitor the drift in the calibration, and occasionally make
3 small adjustments. Generally the drift over the course of weeks was comparable to
4 analytical uncertainty in the measurement (± 1.7 ppb) (Figure 3). However, following a
5 re-tuning of the source parameters after 6 months of heavy use for unrelated experiments
6 the calibration was observed to have changed significantly. Without the re-calibration
7 using the two NOAA standard gases, the inferred N₂O would have been about 25 ppb
8 lower than expected (see open squares in Figure 3). The two-point calibration check is
9 thus essential after any change in the source conditions or after many weeks of analysis.

10
11 The N₂O measurements from the ice core samples proved very effective with a sample
12 reproducibility of ± 4 ppb (1-sigma standard deviation, Table 1), an improvement on
13 previous low-precision mass spectrometric methods and similar to that of gas
14 chromatographic methods (Flückiger et al., 2004) and precise to about 5% relative to the
15 80 ppb glacial-interglacial dynamic range (Schilt et al., 2010). The uncertainty in N₂O
16 measurements from the isotopic fragment propagates into an uncertainty in the isobaric
17 correction of $\pm 0.0045\%$ for $\delta^{13}\text{C-CO}_2$. Additionally, a comparison between the m/z 30
18 reconstruction and an independent N₂O record derived from an N₂O isotopic method on
19 essentially the same samples from the Taylor Glacier archive shows an insignificant
20 mean and 1-sigma standard deviation offset between the two records of only 1 ± 4 ppb
21 (Schilt et al., in revision).

22 **4 Method Performance**

23 **4.1 Linearity**

24 With a dual-inlet system, careful balancing of the capillaries and precise pressure
25 adjustment mitigates most ion source non-linearity. During the periods of analysis, the
26 linearity of the method is demonstrated by relationship between intensity and measured
27 $\delta^{13}\text{C}$ and $\delta^{18}\text{O}$ values relative to the working reference standard (Figure 4). Because the
28 gas for these standard measurements was passed through the gas extraction line, they
29 offer a measure of the overall non-linearity of the system.

30


1 $\delta^{13}\text{C-CO}_2$ increases modestly at about $0.021 \pm 0.008\text{‰}$ per volt and $\delta^{18}\text{O-O}_2$ shows very
2 little trend relative to the noise $0.003 \pm 0.039\text{‰}$ (Figure 4). The standard error of a given
3 measurement (i.e. internal precision) shows a slight trend towards decreased precision
4 with smaller sample size ($\delta^{13}\text{C-CO}_2$ s.e. = -0.0016‰ per volt; $\delta^{18}\text{O-CO}_2$ s.e. = -0.0042‰
5 per volt; both about 20% over mean s.e. per volt).

6
7 Because most measurements fell with a relatively narrow range of major beam intensities
8 ($\sim 2000\text{-}3000$ mV), no non-linearity correction was applied to the data. In the rare
9 instance that the sample size was significantly less than expected (<2000 mV) a series of
10 standard measurements were completed in that range and a separate calibration for the
11 sample was constructed.



13 4.2 Precision


14 Precision is estimated by performing replicate analyses on a selection of samples for the
15 various archives. In the case of WDC05A, the sampling allows for true duplication, that
16 is two samples from the same exact depth. Otherwise, as is the case with WDC06A and
17 Taylor Glacier, duplicates are from adjacent depths (~ 20 cm between mid-depth). Given
18 the degree of gas smoothing in the firn and the depth-age relationship at these sites, the
19 adjacent depths should record nearly identical atmospheric values. For example,
20 assuming a Gaussian gas age distribution with a full width at half maximum of at least 20
21 years and depth/age relationship about 20 cm/year at WAIS Divide (Mitchell, 2013)
22 implies that two gas sample spaced 20 cms apart contain about 95% of the same air.
23 However, variability in the chemistry of the ice is present on these length scales (e.g.
24 annual layers in WDC cores). Replicate analysis from adjacent depths for species that
25 can be subject to in situ production in the ice, most notably of N_2O , could therefore
26 artificially inflate apparent uncertainties.

27
28 The pooled standard deviation of all the $\delta^{13}\text{C-CO}_2$ replicate analyses is 0.018‰ ($n = 23$)
29 (Table 1). This is an improvement of at least 30% on previous dual-inlet methods
30 (reported range from 0.03‰ (Grater 1, $n = 3$) to 0.06‰ (Grater 6, $n = 5$) in Rubino et al.,
31 2013), at least a 60% improvement on the sublimation technique of Schmitt et al., 2011

1 (minimum ~0.05‰) and nearly an order of magnitude better than most of the GC-IRMS
2 techniques. **Parsed by ice archive,**  estimated precisions are very similar (Table 1) and
3 an F-test comparison of the variance in Taylor Glacier and WAIS Divide replicates
4 reveals no statistically significant difference in precision ($p>0.1$).

7 **4.3 Accuracy**

8 **Evaluating the accuracy of ice core gas measurements is a significant challenge,**
9 **primarily because it is impractical to manufacture an artificial ice sample with a known** 
10 **gas composition.** As an alternative, we performed experiments in which a **gas-free** piece
11 of ice (made in the laboratory) is grated along with an aliquot of known NOAA  standard
12 gas; this test examines accuracy after the release of occluded air from ice. When using a
13 standard freezer capable of housing the ice grater at -25°C , we found that standard gas
14 became more depleted in $\delta^{13}\text{C-CO}_2$ than expected when grating the ice or when the ice
15 was warmed in the absence of any grating. This depletion, or "blank" appears to be
16 proportional to the water vapor pressure after air extraction (and by inference the surface
17 temperature of the ice block) (Figure 5).

18
19 After obtaining an ultra-low temperature freezer operated at -60°C , we were able to
20 restrict the water vapor pressure to about 50 mTorr after grating. The reduction of water
21 vapor raised the mean $\delta^{13}\text{C-CO}_2$ value and decreased the scatter in blanks experiments to
22 $-0.066 \pm 0.036\text{‰}$ (1-sigma s.d. $n = 12$) though blanks of up to -0.11‰ were observed on
23 vigorously grated ice blocks (Figure 5). We could not differentiate by experiment
24 whether this effect was dominated by the amount of the water vapor in the grater itself or
25 the flux of water vapor from the ice grater into the extraction line. Based on these
26 experiments we chose to correct all sample measurements assuming a constant blank of
27 $+0.066\text{‰}$. This can be compared to the results of Rubino et al., 2013 which observed
28 blanks of $-0.05 \pm 0.02\text{‰}$ ($n = 4$) and $-0.11 \pm 0.10 \text{‰}$ ($n = 15$) for graters 1 and 6,
29 respectively. By propagating our sample reproducibility ($\pm 0.018\text{‰}$) with the uncertainty
30 in determining the procedural blank ($\pm 0.036\text{‰}$) we estimate the **accuracy**  a single
31 measurement to fall within $\pm 0.04\text{‰}$ (1-sigma s.d.) of the NOAA scale if these errors are

1 uncorrelated. For comparison, the same metric would suggest that the Rubino et al., 2013
2 method should fall within ± 0.036 and $\pm 0.12\%$ of the CSIRO scale for grater 1 and 6,
3 respectively.

5 Oxygen Isotopic Fractionation

6 The oxygen isotopic composition of atmospheric CO₂ is primarily controlled by the
7 exchange of oxygen between CO₂ and H₂O during photosynthesis in plant leaves and
8 respiration in soils. Atmospheric $\delta^{18}\text{O-CO}_2$ therefore offers a constraint on gross of
9 primary production and the hydrological cycle on a global scale (Welp et al., 2011).
10 However, the atmospheric signal of $\delta^{18}\text{O-CO}_2$ in ice core gas is probably compromised
11 by exchange of oxygen with the surrounding ice (Friedli et al., 1984). The process by
12 which this exchange occurs is somewhat enigmatic as it most likely requires the
13 interaction of CO₂ and liquid water at sub-freezing temperatures. Though liquid water in
14 very small amounts is probably ubiquitous in polar ice, specifically at the triple junctions
15 of grains (Mader, 1992; Nye and Frank, 1973), its influence on the preservation of gas
16 records is not well known. A better understanding of the interaction of gas and ice is
17 important for constraining any possible diffusion of atmospheric signals in the very old
18 (>1 million years ago) and very warm basal ice that may be recovered as part of “Oldest
19 Ice” project (Fischer et al., 2013).

20
21 Observations of ice core $\delta^{18}\text{O-CO}_2$ have previously been reported and discussed from
22 low-resolution measurements from ice cores at Siple Dome, South Pole and Byrd
23 ((Siegenthaler et al., 1988); hereafter *Siegenthaler*) and high-precision measurements
24 from firn sampling campaigns at Dome C, Dronning Maud Land, and Berkner Island
25 ((Assonov et al., 2005); hereafter *ABJ*). *Siegenthaler* observed $\delta^{18}\text{O-CO}_2$ values about 20
26 to 30‰ more depleted than typical atmospheric values and correlated to the variations of
27 $\delta^{18}\text{O}$ in the surrounding ice matrix. *ABJ* also observed $\delta^{18}\text{O-CO}_2$ becoming more depleted
28 relative to the atmosphere as the age of the CO₂ increases with depth in the firn.

29
30 We too observe very highly correlated $\delta^{18}\text{O-CO}_2$ and $\delta^{18}\text{O-H}_2\text{O}$ (Figures 6 and 7). Most
31 notably, the high (~3 cm) resolution $\delta^{18}\text{O-H}_2\text{O}$ data from the WDC05A core (Steig et al.,

1 2013) allows us to accurately determine the mean $\delta^{18}\text{O}$ surrounding each gas sample
 2 (Figure 6). $\delta^{18}\text{O}$ - H_2O measurements from Taylor Glacier (Daniel Baggenstos, personal
 3 communication) are only available in nearby samples so the $\delta^{18}\text{O}$ - H_2O data was
 4 smoothed and interpolated before comparison with the gas data. The apparent
 5 fractionation (ϵ) between CO_2 and H_2O is determined by taking the difference between
 6 $\delta^{18}\text{O}$ - CO_2 and $\delta^{18}\text{O}$ - H_2O on a sample-by-sample basis. Note that $\epsilon_{a-b} = 1000 \ln(\alpha_{a-b}) \approx \delta_a -$
 7 δ_b .

8

9 The mean and 1-sigma standard deviation of the apparent $\epsilon(\text{CO}_2\text{-H}_2\text{O}_{(s)})$ is 47.43 ± 0.45
 10 and $44.42 \pm 1.34\text{‰}$, for WDC05A and Taylor Glacier, respectively (Table 3). With the
 11 *in situ* ice temperature of WDC05A about 11 K colder than Taylor Glacier, there appears
 12 to be an increase in fractionation with decreasing temperature. The higher noise in the
 13 Taylor Glacier $\delta^{18}\text{O}$ - CO_2 data is probably related to the aliasing of high-frequency $\delta^{18}\text{O}$ -
 14 H_2O variability.

15

16 The $\epsilon(\text{CO}_2\text{-H}_2\text{O}_{(s)})$ show no discernible trend with time. Even the youngest sample at
 17 WAIS Divide (gas age = 1915 C.E.) is only about 1‰ heavier than the mean $\epsilon(\text{CO}_2\text{-}$
 18 $\text{H}_2\text{O}_{(s)})$ for the entire core, appearing to be mostly equilibrated with the surrounding ice.
 19 This is consistent with the observation of the rate of exchange in the firn. *ABJ* calculate
 20 the equilibration proceeds with a half-life of about 23 years at the Berkner Island Site,
 21 which at -26°C is only slightly warmer than WAIS Divide, suggesting that youngest
 22 WAIS Divide sample should be about 90% equilibrated.

23

24 *Siegenthaler* proposed that apparent fractionation between the ice matrix and gaseous
 25 CO_2 , could be described by temperature dependent fractionation at thermodynamic
 26 equilibrium between gaseous CO_2 and the solid, liquid and vapor phases of the H_2O as
 27 follows:

28

$$29 \quad \alpha(\text{CO}_2 - \text{H}_2\text{O}_{(s)}) = \alpha(\text{CO}_2 - \text{H}_2\text{O}_{(l)})\alpha(\text{H}_2\text{O}_{(l)} - \text{H}_2\text{O}_{(g)})\alpha(\text{H}_2\text{O}_{(g)} - \text{H}_2\text{O}_{(s)}) \quad (1)$$

30

1 The left hand side of the equation is the expected fractionation between gaseous CO₂ and
2 solid water — what we would expect to see in the ice core. The fractionation factors on
3 the right hand side of the equation have been estimated by theoretical and experimental
4 work, but $\alpha(\text{CO}_2\text{-H}_2\text{O}_{(l)})$ and $\alpha(\text{H}_2\text{O}_{(l)}\text{-H}_2\text{O}_{(g)})$ have not been determined below the
5 freezing point of water. The $\alpha(\text{H}_2\text{O}_{(g)}\text{-H}_2\text{O}_{(s)})$ has been determined over a wide range of
6 sub-freezing temperatures because of its relevance in interpreting oxygen isotope records
7 from polar ice but is not well-constrained at very cold temperatures ($\sim < 240$ K).

8
9 *Siegenthaler* used $\alpha(\text{CO}_2\text{-H}_2\text{O}_{(l)})$ from Bottinja, 1968 and $\alpha(\text{H}_2\text{O}_{(l)}\text{-H}_2\text{O}_{(g)})$ and $\alpha(\text{H}_2\text{O}_{(g)}\text{-}$
10 $\text{H}_2\text{O}_{(s)})$ from Majoube, 1971 (Table 4 summarizes these and other fractionation factors,
11 and provides shorthand for the formulations). Using the fractionation factors from
12 *Siegenthaler*, we find our $\delta^{18}\text{O}\text{-CO}_2$ values are 1.19 ± 0.45 and $1.58 \pm 1.34\%$ ‰
13 depleted than would be expected from complete equilibration in WAIS Divide and Taylor
14 Glacier, respectively (Table 3). Given the uncertainties in determining the apparent
15 fractionation from the noisy data and accurately measuring $\delta^{18}\text{O}\text{-CO}_2$, the new data are
16 mostly in agreement with previous data and proposed model for $\delta^{18}\text{O}\text{-CO}_2$ equilibration
17 (Figure 8).

18
19 The uncertainties in the ice core data, however, are smaller than the uncertainties in other
20 experimentally and theoretically derived estimates of temperature dependent
21 fractionation. Including additional estimates suggests that the predicted $\alpha(\text{CO}_2\text{-H}_2\text{O}_{(s)})$ is
22 relatively insensitive to changing $\alpha(\text{CO}_2\text{-H}_2\text{O}_{(l)})$ and $\alpha(\text{H}_2\text{O}_{(l)}\text{-H}_2\text{O}_{(g)})$ (black band, Figure
23 8). However, the convergence of the expected fractionation from various studies does
24 not necessarily equate to accuracy because these formulations are extrapolated below the
25 freezing point. On the other hand, $\alpha(\text{CO}_2\text{-H}_2\text{O}_{(s)})$ appears very sensitive to different
26 $\alpha(\text{H}_2\text{O}_{(g)}\text{-H}_2\text{O}_{(s)})$ predictions from experimental observations (Ellehoj et al., 2013;
27 Majoube, 1971) and theoretical work (Méheut et al., 2007), showing a divergence at very
28 cold temperatures (dot and dash-dot lines, Figure 8) that is larger than the error in the ice
29 core measurements. Though $\alpha(\text{H}_2\text{O}_{(g)}\text{-H}_2\text{O}_{(s)})$ can probably be better constrained by
30 controlled experiments in the laboratory, ice core $\delta^{18}\text{O}\text{-CO}_2$ may offer a unique, natural
31 experiment to observe this process over long time periods, warranting further work.

1
2 Finally, by combining our data with the results from *Siegenthaler*, we derive a
3 relationship for $\alpha(\text{CO}_2\text{-H}_2\text{O}_{(s)})$ and temperature with the form:

4
5
$$\varepsilon = 1000 \ln(\alpha) = \frac{K_2(10^6)}{T^2} - \frac{K_1(10^3)}{T} + K_0 \quad (2)$$

6
7 With temperature in absolute degrees, $K_2 = 19.5 \pm 27.6$, $K_1 = -145 \pm 226$ and $K_0 = 312 \pm 461$.
8 The relationship remains under constrained (light grey band in Figure 8 shows 95% C.I.
9 of the fit). Additional data from ice archives with different temperature, especially at sites
10 with very cold temperatures, would narrow the uncertainty in these coefficients.

11 12 **6 Conclusions**

13 The method presented here advances the methodology for measuring the $\delta^{13}\text{C-CO}_2$ from
14 polar ice. The external precision of $\pm 0.018\%$ and accuracy of $\pm 0.04\%$ obtained by dual-
15 inlet mass spectrometry is an improvement on most other methods. To put this some
16 perspective, this method can resolve isotopic variations of about 6% or the total glacial-
17 interglacial range of $\delta^{13}\text{C-CO}_2$ ($\sim 0.3\%$), which is essential for understanding carbon
18 cycle dynamics. Also, very fast inputs of terrestrial carbon to the atmosphere (signature
19 of about $\sim -0.03\%$ per ppm CO_2) can be delineated for CO_2 variations of less than 3 ppm.

20
21 This study describes the rigorous testing and careful analytical procedures, including
22 source tuning, linearity testing, and daily calibration that are required to obtain high-
23 precision with a dual-inlet technique on very small samples (~ 1.5 bar μL). By
24 demonstrating a method for accurately correcting for isobaric interference of N_2O on
25 small sample, a significant barrier for dual-inlet measurement of ice core or other limited
26 atmospheric sampling studies of CO_2 has been surmounted. Our dual-inlet method
27 provides a means for determining the CO_2 and N_2O mixing ratios on the same ancient air
28 sample, given sufficiently large ice samples. Finally, the $\delta^{18}\text{O-CO}_2$ data presented here
29 constrain the fractionation of oxygen isotopes during what appears to be an exchange of

1 oxygen between CO₂ and solid ice. Future methodological improvements should focus
2 on increasing the grating efficiency to make the method suitable for clathrated ice.

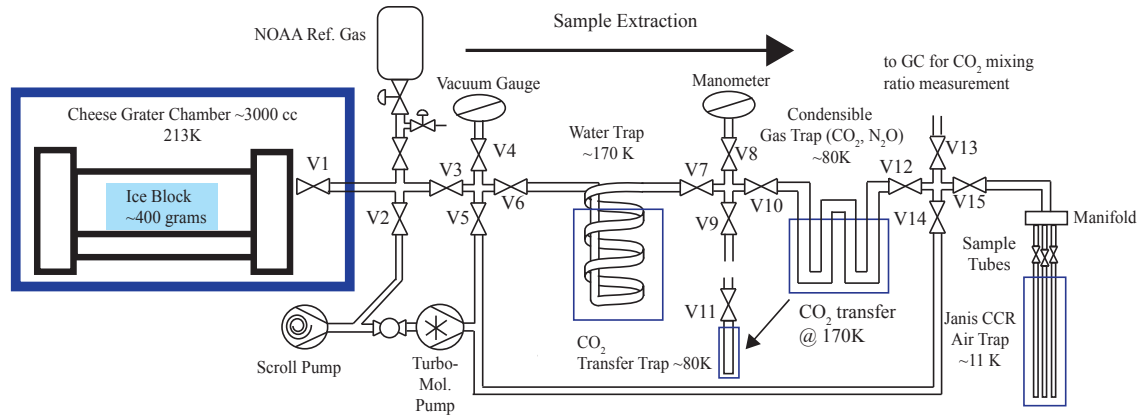
3

4 **7 Acknowledgements**

5 This work was supported by NSF Grant 0839078 (EJB and ACM). Oregon State
6 University provided additional support for mass spectrometer purchase and management
7 of the OSU/CEOAS stable isotope laboratory. We thank the WAIS Divide Science
8 Coordination Office for the collection and distribution of the WAIS Divide ice core
9 (Kendrick Taylor (Desert Research Institute of Reno Nevada), NSF Grants 0230396,
10 0440817, 0944348; and 0944266 - University of New Hampshire) and the Taylor Glacier
11 2010-2011 Field Team (Daniel Baggenstos, James Lee, Hinrich Schaefer, Tanner Kuhl,
12 Robb Kulin, Jeff Severinghaus, Vas Petrenko and Paul Rose) for collection of Taylor
13 Glacier samples with support from NSF Grant 0838936 (EJB). We also appreciate
14 comments provided by R. H. Rhodes on an earlier version of this manuscript.

15

1

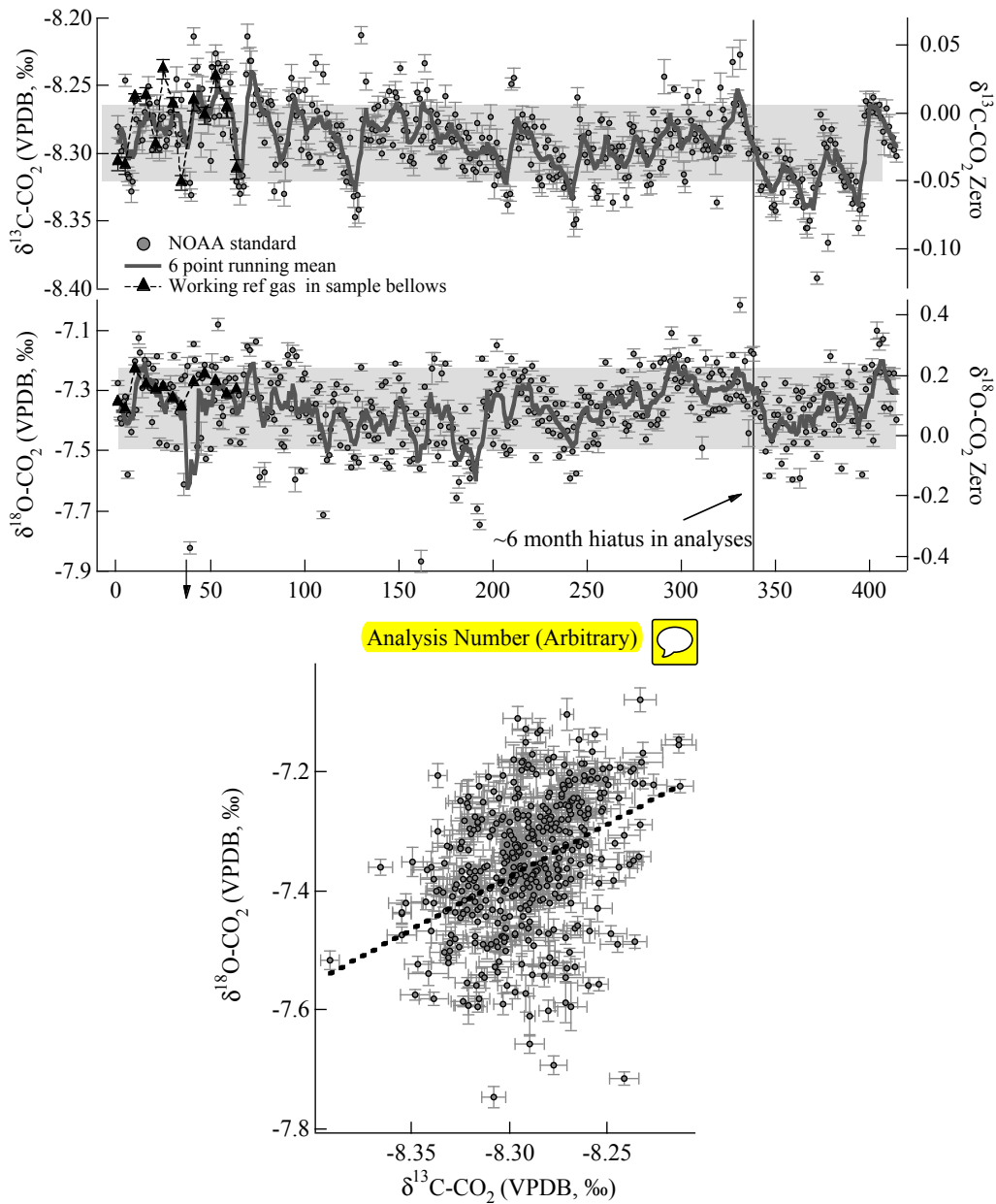


2

3 **Figure 1 Extraction Line**

4 A simplified schematic of the ice core air extraction vacuum line.

5

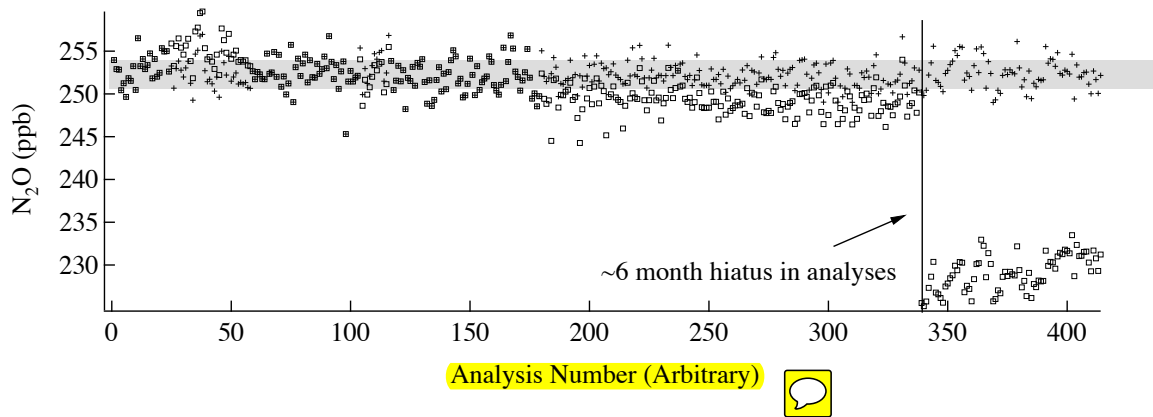


1

2 **Figure 2 Standard Measurement Reproducibility**

3 Upper Panel: All measurements of the NOAA1 standard gas over the course of a number
 4 of measurement campaigns encompassing about 5 months time in total. The $\delta^{13}\text{C}$ and
 5 $\delta^{18}\text{O}-\text{CO}_2$ are reported relative to the working reference gas. Analyses of the working
 6 reference gas stored in the sample bellows (black triangles) (plotted on the “zero” axis).
 7 The gray bars represent the 1-sigma standard deviation of the NOAA1 standard over the
 8 entire period. Lower Panel: $\delta^{13}\text{C}-\text{CO}_2$ covariation with $\delta^{18}\text{O}-\text{CO}_2$ ($R^2 = 0.13$).

1



2

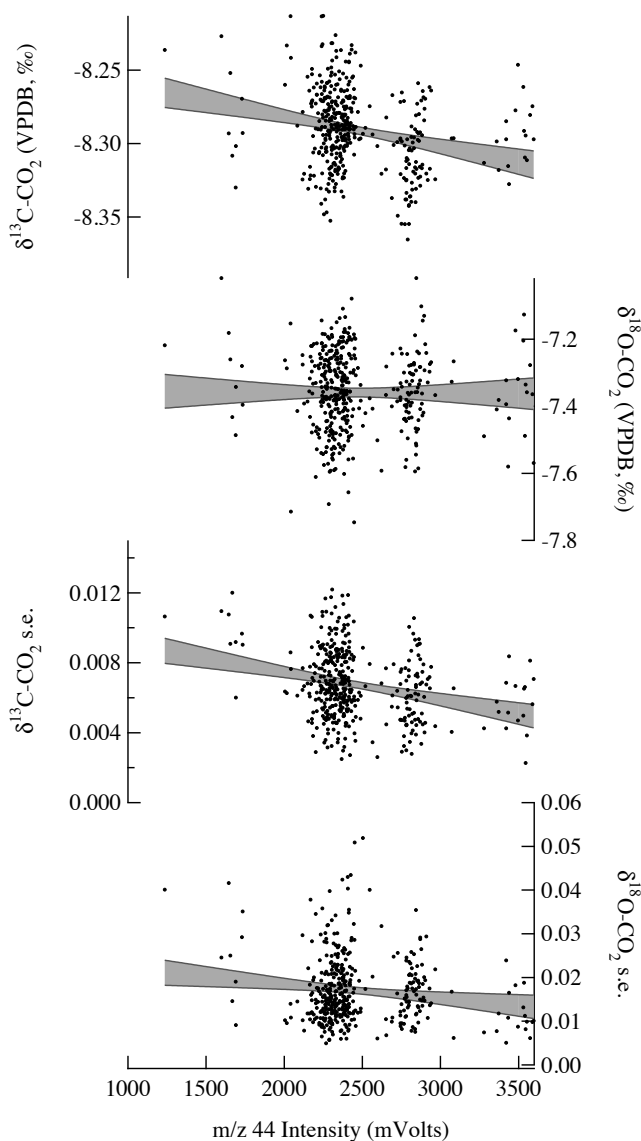
3 **Figure 3 N₂O Standard Reproducibility**

4 The reproducibility and drift in the N₂O calibration of the same period of analysis as in
5 Figure 2. The black crosses are the N₂O of the NOAA1 standard as determined by the
6 daily calibration. The open squares represent the same data if the calibration was fixed to
7 a set value at the beginning of analysis (time 0). This shows both a small drift from about
8 number 0 to 300 (~4 months) and a major shift in the values around 340, which
9 represents a 6 month hiatus and re-tuning of the ion source.

10

11

1



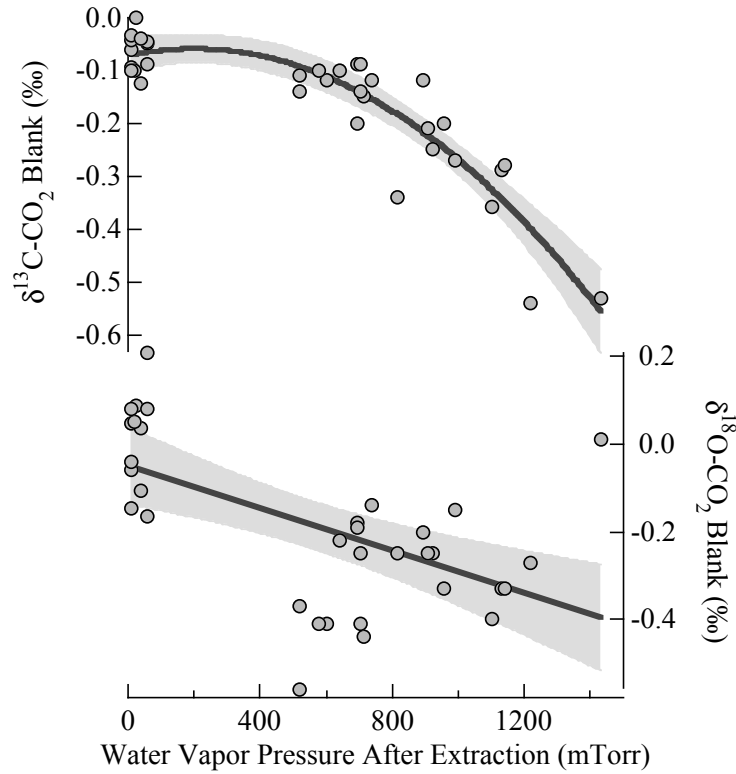
2

3 **Figure 4 Linearity and Precision of Standard Measurements**

4 The linearity and internal precision of the measurement versus m/z 44 intensity as
5 recorded by measurements of the NOAA1 standard during the period of analysis. $\delta^{13}\text{C}$
6 and $\delta^{18}\text{O-CO}_2$ are reported relative to the working reference gas (upper two panels) and
7 the internal precision is reported as 1-sigma standard error of the eight dual-inlet
8 measurements (lower two panels). The grey shading represents the 95% confidence
9 intervals for a linear fit to the data.

10

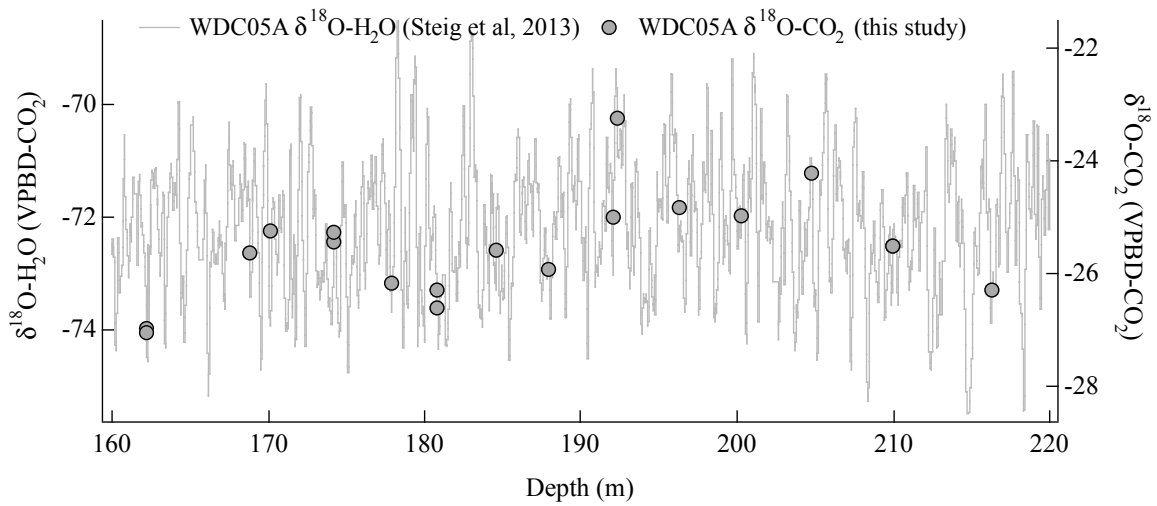
1
2
3



4 **Figure 5 Procedural Blank Experiments**

5 Measurements of the procedural blank of the system and its relationship to water vapor
6 pressure. Blank is reported as the difference of the expected δ -value (from the NOAA
7 calibration) to the measured value when ice grating and air extraction is simulated.
8 Negative blanks indicate that the standard air become more negative during the
9 simulation. The grey shading indicates 3rd order polynomial fit to the $\delta^{13}\text{C-CO}_2$ with 95%
10 confidence intervals and linear fit to the $\delta^{18}\text{O-CO}_2$.

11
12
13
14



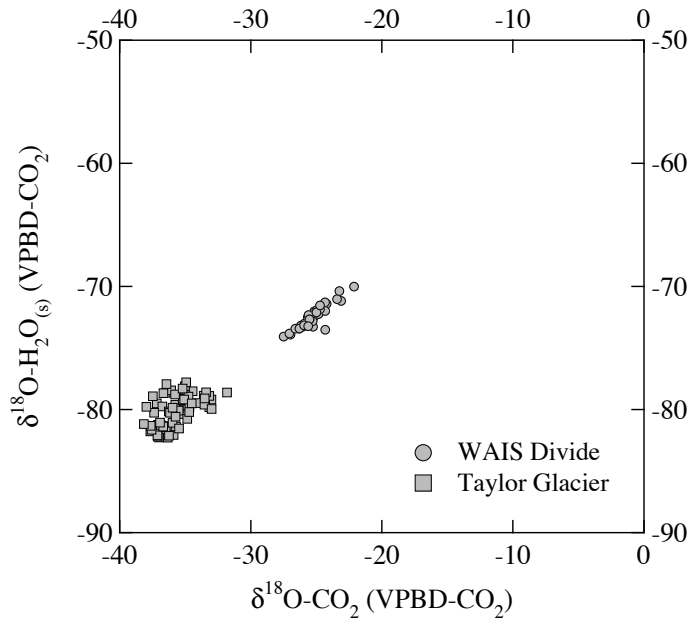
1

2 **Figure 6 WAIS Divide $\delta^{18}\text{O-CO}_2$ and $\delta^{18}\text{O-H}_2\text{O}$**

3 A short selection of the $\delta^{18}\text{O-CO}_2$ (this study) and $\delta^{18}\text{O-H}_2\text{O}$ data (Steig et al., 2013) on
 4 the depth scale from the WDC05A core. The two vertical axes are of the same
 5 magnitude but offset to show the ability of $\delta^{18}\text{O-CO}_2$ to capture and integrate the fine
 6 scale $\delta^{18}\text{O-H}_2\text{O}$.

7

8

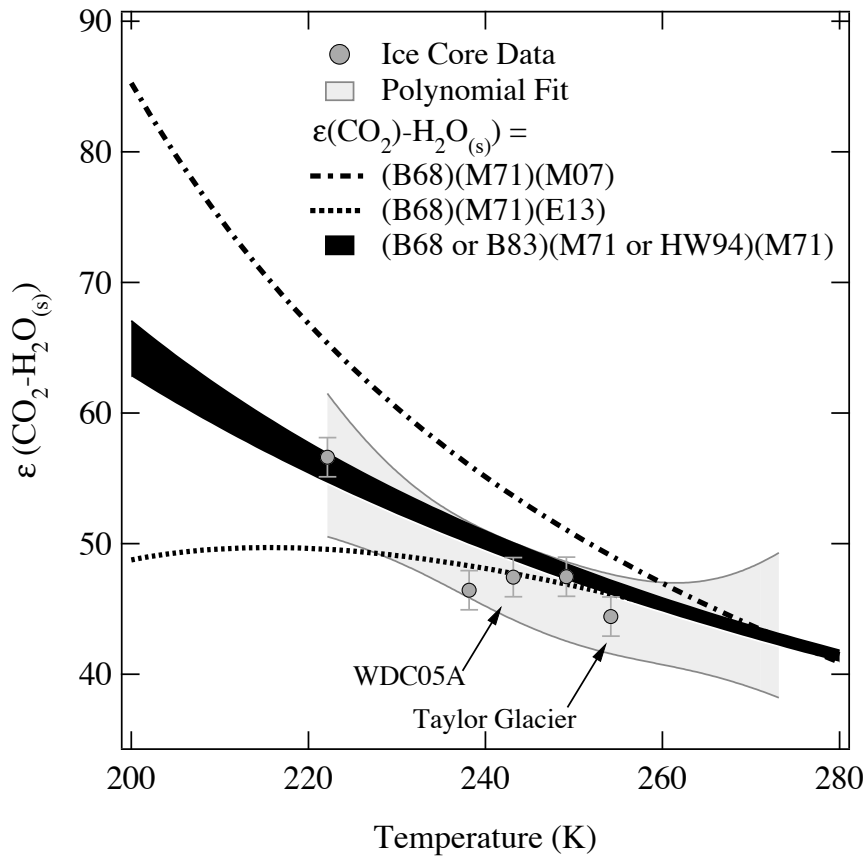


1
2
3
4
5

Figure 7 $\delta^{18}\text{O}-\text{CO}_2$ and $\delta^{18}\text{O}-\text{H}_2\text{O}$ correlation

$\delta^{18}\text{O}-\text{CO}_2$ plotted against $\delta^{18}\text{O}-\text{H}_2\text{O}$ from the WAIS Divide and Taylor Glacier archives.

1
2



3
4
5
6
7
8
9
10
11
12
13
14
15

Figure 8 Temperature dependence of oxygen isotope fractionation

The relationship between ice core $\delta^{18}\text{O}\text{-CO}_2$ gas fractionation $\epsilon(\text{CO}_2\text{-H}_2\text{O}_{(s)})$ (grey circles) from this study (indicated with arrows) and Siegenthaler et al., 1988. The light grey shading indicates a 3rd order polynomial fit to the data. The curves indicated the predicted fraction in thermodynamic equilibrium of gaseous CO_2 with vapor, liquid and solid H_2O (Equation 1). The black banding uses a range of determinations for $\alpha(\text{CO}_2\text{-H}_2\text{O}_{(l)})$ and $\alpha(\text{H}_2\text{O}_{(l)}\text{-H}_2\text{O}_{(g)})$ but only M71 for $\alpha(\text{H}_2\text{O}_{(g)}\text{-H}_2\text{O}_{(s)})$. The dot-dashed line uses only B68 for $\alpha(\text{CO}_2\text{-H}_2\text{O}_{(l)})$ and M71 for $\alpha(\text{H}_2\text{O}_{(l)}\text{-H}_2\text{O}_{(g)})$ but M07 for $\alpha(\text{H}_2\text{O}_{(g)}\text{-H}_2\text{O}_{(s)})$. The dotted line also uses only B68 for $\alpha(\text{CO}_2\text{-H}_2\text{O}_{(l)})$ and M71 for $\alpha(\text{H}_2\text{O}_{(l)}\text{-H}_2\text{O}_{(g)})$ but E13 for $\alpha(\text{H}_2\text{O}_{(g)}\text{-H}_2\text{O}_{(s)})$ (See Table 4 for a description of the fractionation formulas).

1
2
3

Table 1 Ice archives utilized in this study with their respective precisions from replicate analysis

Ice Archive	Drill Fluid	Type of Replicates	n	1-sigma pooled standard deviation of replicate analyses		
				$\delta^{13}\text{C-CO}_2$ (‰)	CO_2 (ppm)	N_2O (ppb)
WDC05A	none	true	8	0.016	2.18	3.83
WDC06A	Isopar-K, HCFC-141b	adjacent depths	6	0.014	1.04	2.4
Taylor Glacier	none	adjacent depths	9	0.022	1.3	5.23
Overall			23	0.018	1.9	4.35

4
5

1
2
3

Table 2 Gas concentrations and nominal isotopic composition of reference gases.

	Mixing Ratio			Isotopic Composition			
	Reference Scale	CO ₂ (ppm) (s.d)	N ₂ O (ppb) (s.d)	Analysis Facility	Primary Ref. Material	δ ¹³ C-CO ₂ (VPDB-CO ₂)	δ ¹⁸ O-CO ₂ (VPDB-CO ₂)
NOAA1	2007 WMO MOLE FRACTION SCALE (CO ₂), NOAA-2006 (N ₂ O)	277.04 (0.03)	252.6 (0.2)	INSTAAR-SIL	NBS-19	-8.288	-7.171
				OSU	NBS-19	-8.287	-7.58
NOAA2	SCALE (CO ₂), NOAA-2006 (N ₂ O)	150.01 (0.01)	321.96 (0.2)	INSTAAR-SIL	NBS-19	-8.135	-0.578
				OSU	NBS-19	-8.101	-0.934
Working Ref.	n.a.	pure	n.a.	Oztech		-10.39	-9.84
				OSU	NBS-19	-10.51	-10.06

4
5
6

1
2

Table 3 Observed $\delta^{18}\text{O}$ of CO_2 fractionation results from this study and other studies

Core	Study	Age Interval	$\delta^{18}\text{O}\text{-CO}_2$ (VPD- CO_2)	$\delta^{18}\text{O}\text{-H}_2\text{O}$ (VPD- CO_2)	Temp. (K)	$\epsilon_{\text{CO}_2\text{-H}_2\text{O}}$ (Observed)
WAIS Divide	this study	1.25-0.1 ka	-25.17	-72.41	243	47.43±0.45
Taylor Glacier		23-11 ka	-35.58	-80.00	254	44.42±1.34
Siple Dome	(Siegenthaler et al., 1988)	0.3-0.1 ka	-20.40	-67.86	249	47.46
South Pole		0.9-0.4 ka	-31.70	-88.31	222	56.61
Byrd		~50 ka	-31.80	-78.23	238	46.43

3
4
5

1
2
3
4
5

6

Table 4 $\delta^{18}\text{O}$ Fractionation Factors

$\alpha(\text{A-B})$	$1000 \ln(\alpha) =$	Reference	Short-hand
$\alpha(\text{CO}_2\text{-H}_2\text{O}_{(\text{l})})$	$-\frac{0.021(10^6)}{T^2} + \frac{17.99(10^3)}{T} - 19.97$	(Bottinga and Craig, 1968)	B68
	$\frac{17.6(10^3)}{T} - 17.93$	(Brenninkmeijer et al., 1983)	B83
$\alpha(\text{H}_2\text{O}_{(\text{l})}\text{-H}_2\text{O}_{(\text{g})})$	$\frac{1.137(10^6)}{T^2} - \frac{0.42(10^3)}{T} - 2.07$	(Majoube, 1971)	M71
	$\frac{0.35(10^9)}{T^3} - \frac{1.666(10^6)}{T^2} + \frac{6.71(10^3)}{T} - 7.68$	(Horita and Wesolowski, 1994)	HW94
$\alpha(\text{H}_2\text{O}_{(\text{s})}\text{-H}_2\text{O}_{(\text{g})})$	$\frac{11.84(10^3)}{T} - 28.22$	(Majoube, 1971)	M71
	$-0.0016799x^3 - .00721x^2 + 1.675x - 2.685$ where $x = \frac{10^6}{T^2}$	(Méheut et al., 2007)	M07
	$\left(\frac{8312.5}{T^2} - \frac{49.192}{T} + 0.0831\right) \times 1000$	(Ellehoj et al., 2013)	E13

1

2 **References**

- 3 Ahn, J., Brook, E. J. and Howell, K.: A high-precision method for measurement of
4 paleoatmospheric CO₂ in small polar ice samples, *J. Glaciol.*, 55(191), 499–506, 2009.
- 5 Assonov, S. S. and Brenninkmeijer, C. A. M.: On the N₂O correction used for mass
6 spectrometric analysis of atmospheric CO₂, *Rapid Commun. Mass Spectrom.*, 20(11),
7 1809–1819, doi:10.1002/rcm.2516, 2006.
- 8 Assonov, S. S., Brenninkmeijer, C. A. M. and Jöckel, P.: The ¹⁸O isotope exchange rate
9 between firm air CO₂ and the firm matrix at three Antarctic sites, *J. Geophys. Res.*
10 *Atmospheres*, 110(D18), 2005.
- 11 Bottinga, Y. and Craig, H.: Oxygen isotope fractionation between CO₂ and water, and the
12 isotopic composition of marine atmospheric CO₂, *Earth Planet. Sci. Lett.*, 5, 285–295,
13 1968.
- 14 Brenninkmeijer, C. A. M., Kraft, P. and Mook, W. G.: Oxygen Isotope Fractionation
15 Between CO₂ and H₂O, *Isot. Geosci.*, 1(2), 181–190, 1983.
- 16 Ellehoj, M. D., Steen-Larsen, H. C., Johnsen, S. J. and Madsen, M. B.: Ice-vapor
17 equilibrium fractionation factor of hydrogen and oxygen isotopes: Experimental
18 investigations and implications for stable water isotope studies, *Rapid Commun. Mass*
19 *Spectrom.*, 27(19), 2149–2158, doi:10.1002/rcm.6668, 2013.
- 20 Elsig, J., Schmitt, J., Leuenberger, D., Schneider, R., Eyer, M., Leuenberger, M., Joos, F.,
21 Fischer, H. and Stocker, T. F.: Stable isotope constraints on Holocene carbon cycle
22 changes from an Antarctic ice core, *Nature*, 461(7263), 507–510,
23 doi:10.1038/nature08393, 2009.
- 24 Fischer, H., Severinghaus, J., Brook, E., Wolff, E., Albert, M., Alemany, O., Arthern, R.,
25 Bentley, C., Blankenship, D., Chappellaz, J., Creyts, T., Dahl-Jensen, D., Dinn, M.,
26 Frezzotti, M., Fujita, S., Gallee, H., Hindmarsh, R., Hudspeth, D., Jugie, G., Kawamura,
27 K., Lipenkov, V., Miller, H., Mulvaney, R., Pattyn, F., Ritz, C., Schwander, J., Steinhage,
28 D., van Ommen, T. and Wilhelms, F.: Where to find 1.5 million yr old ice for the IPICS
29 “Oldest Ice” ice core, *Clim Past Discuss*, 9(3), 2771–2815, doi:10.5194/cpd-9-2771-
30 2013, 2013.
- 31 Flückiger, J., Blunier, T., Stauffer, B., Chappellaz, M., Spahni, R., Kawamura, K.,
32 Schwander, J., Stocker, T. F. and Dahl-Jensen, D.: N₂O and CH₄ variations during the
33 last glacial epoch: Insight into global processes, *Glob. Biogeochem. Cycles*, 18(1)
34 [online] Available from: [://000188866700004](https://doi.org/10.1029/2000188866700004), 2004.
- 35 Francey, R. J., Allison, C. E., Etheridge, D. M., Trudinger, C. M., Enting, I. G.,
36 Leuenberger, M., Langenfelds, R. L., Michel, E. and Steele, L. P.: A 1000-year high

- 1 precision record of $\delta^{13}\text{C}$ in atmospheric CO_2 , *Tellus B*, 51(2), 170–193,
2 doi:10.1034/j.1600-0889.1999.t01-1-00005.x, 1999.
- 3 Friedli, H., Moor, E., Oeschger, H., Siegenthaler, U. and Stauffer, B.: $^{13}\text{C}/^{12}\text{C}$ ratios in
4 CO_2 extracted from Antarctic ice, *Geophys. Res. Lett.*, 11(11), 1145–1148,
5 doi:10.1029/GL011i011p01145, 1984.
- 6 Friedli, H. and Siegenthaler, U.: Influence of N_2O on isotope analyses in CO_2 and mass-
7 spectrometric determination of N_2O in air samples, *Tellus B*, 40B(2), 129–133,
8 doi:10.1111/j.1600-0889.1988.tb00216.x, 1988.
- 9 Friedli, H. and Stauffer, B.: Ice core record of the $^{13}\text{C}/^{12}\text{C}$ ratio of atmospheric CO_2 , in
10 the past two centuries, *Nature*, 324(20), 237–238, 1986.
- 11 Halsted, R. E. and Nier, A. O.: Gas Flow through the Mass Spectrometer Viscous Leak,
12 *Rev. Sci. Instrum.*, 21(12), 1019–1021, doi:10.1063/1.1745483, 1950.
- 13 Horita, J. and Wesolowski, D. J.: Liquid-vapor fractionation of oxygen and hydrogen
14 isotopes of water from the freezing to the critical temperature, *Geochim. Cosmochim.*
15 *Acta*, 58(16), 3425–3437, 1994.
- 16 Indermuhle, A., Stocker, T. F., Joos, F., Fischer, H., Smith, H. J., Wahlen, M., Deck, B.,
17 Mastoianni, D., Tschumi, J., Blunier, T., Meyer, R. and Stauffer, B.: Holocene carbon-
18 cycle dynamics based on CO_2 trapped in ice at Taylor Dome, Antarctica, *Nature*,
19 398(6723), 121–126, 1999.
- 20 Leuenberger, M. C., Eyer, M., Nyfeler, P., Stauffer, B. and Stocker, T. F.: High-
21 resolution delta C-13 measurements on ancient air extracted from less than 10 cm(3) of
22 ice, *Tellus Ser. B-Chem. Phys. Meteorol.*, 55(2), 138–144, 2003.
- 23 Leuenberger, M., Siegenthaler, U. and Langway, C. C.: Carbon isotope composition of
24 atmospheric CO_2 during the last ice-age from an Antarctic ice core, *Nature*, 357(6378),
25 488–490, 1992.
- 26 Lourantou, A., Lavric, J. V., Kohler, P., Barnola, J. M., Paillard, D., Michel, E., Raynaud,
27 D. and Chappellaz, J.: Constraint of the CO_2 rise by new atmospheric carbon isotopic
28 measurements during the last deglaciation, *Glob. Biogeochem. Cycles*, 24,
29 doi:10.1029/2009gb003545, 2010.
- 30 Mader, H. M.: Observations of the water-vein system in polycrystalline ice, *J. Glaciol.*,
31 38(130), 333–347, 1992.
- 32 Majoube, M.: Oxygen-18 and Deuterium Fractionation Between Water and Steam, *J.*
33 *Chim. Phys. Phys.-Chim. Biol.*, 68(10), 1423–1436, 1971.
- 34 Masarie, K. A., Langenfelds, R. L., Allison, C. E., Conway, T. J., Dlugokencky, E. J.,
35 Francey, R. J., Novelli, P. C., Steele, L. P., Tans, P. P., Vaughn, B. and White, J. W. C.:
36 NOAA/CSIRO Flask Air Intercomparison Experiment: A strategy for directly assessing

- 1 consistency among atmospheric measurements made by independent laboratories, J.
2 Geophys. Res. Atmospheres, 106(D17), 20445–20464, doi:10.1029/2000JD000023,
3 2001.
- 4 Méheut, M., Lazzeri, M., Balan, E. and Mauri, F.: Equilibrium isotopic fractionation in
5 the kaolinite, quartz, water system: Prediction from first-principles density-functional
6 theory, *Geochim. Cosmochim. Acta*, 71(13), 3170–3181, doi:10.1016/j.gca.2007.04.012,
7 2007.
- 8 Mitchell, L. E.: *The Late Holocene Atmospheric Methane Budget Reconstructed from Ice*
9 *Cores*, Oregon State University, Corvallis, OR, Winter., 2013.
- 10 Mitchell, L. E., Brook, E. J., Sowers, T., McConnell, J. R. and Taylor, K.: Multidecadal
11 variability of atmospheric methane, 1000-1800 CE, *J. Geophys. Res.-Biogeosciences*,
12 116, doi:10.1029/2010jg001441, 2011.
- 13 Miteva, V., Sowers, T. and Brenchley, J.: Production of N₂O by Ammonia Oxidizing
14 Bacteria at Subfreezing Temperatures as a Model for Assessing the N₂O Anomalies in
15 the Vostok Ice Core, *Geomicrobiol. J.*, 24(5), 451–459,
16 doi:10.1080/01490450701437693, 2007.
- 17 Nye, J. F. and Frank, F. C.: Hydrology of the intergranular veins in a temperate glacier, in
18 *Symposium on the Hydrology of Glaciers*, vol. 95, pp. 157–161., 1973.
- 19 Rubino, M., Etheridge, D. M., Trudinger, C. M., Allison, C. E., Battle, M. O.,
20 Langenfelds, R. L., Steele, L. P., Curran, M., Bender, M., White, J. W. C., Jenk, T. M.,
21 Blunier, T. and Francey, R. J.: A revised 1000 year atmospheric $\delta^{13}\text{C}$ -CO₂ record from
22 Law Dome and South Pole, Antarctica, *J. Geophys. Res. Atmospheres*, 118(15), 8482–
23 8499, doi:10.1002/jgrd.50668, 2013.
- 24 Santrock, J., Studley, S. A. and Hayes, J. M.: Isotopic analyses based on the mass-
25 spectrum of carbon-dioxide, *Anal. Chem.*, 57(7), 1444–1448, doi:10.1021/ac00284a060,
26 1985.
- 27 Schaefer, H., Lourantou, A., Chappellaz, J., Lüthi, D., Bereiter, B. and Barnola, J.-M.: On
28 the suitability of partially clathrated ice for analysis of concentration and $\delta^{13}\text{C}$ of palaeo-
29 atmospheric CO₂, *Earth Planet. Sci. Lett.*, 307(3–4), 334–340,
30 doi:10.1016/j.epsl.2011.05.007, 2011.
- 31 Schilt, A., Baumgartner, M., Blunier, T., Schwander, J., Spahni, R., Fischer, H. and
32 Stocker, T. F.: Glacial–interglacial and millennial-scale variations in the atmospheric
33 nitrous oxide concentration during the last 800,000 years, *Clim. Last Million Years New*
34 *Insights EPICA Rec.*, 29(1–2), 182–192, doi:10.1016/j.quascirev.2009.03.011, 2010.
- 35 Schilt, A., Brook, E. J., Bauska, T. K., Baggenstos, D., Fischer, H., Joos, F., Petrenko, V.
36 V., Schaefer, H., Schmitt, J., Severinghaus, J. P., Spahni, R. and Stocker, T. F.: Isotopic
37 constraints on marine and terrestrial N₂O emissions during the last deglaciation, *Nature*, in
38 review.

- 1 Schmitt, J., Schneider, R., Elsig, J., Leuenberger, D., Lourantou, A., Chappellaz, J.,
2 Koehler, P., Joos, F., Stocker, T. F., Leuenberger, M. and Fischer, H.: Carbon Isotope
3 Constraints on the Deglacial CO₂ Rise from Ice Cores, *Science*, 336(6082), 711–714,
4 doi:10.1126/science.1217161, 2012.
- 5 Schmitt, J., Schneider, R. and Fischer, H.: A sublimation technique for high-precision
6 measurements of $\delta^{13}\text{CO}_2$ and mixing ratios of CO₂ and N₂O from air trapped in ice cores,
7 *Atmos Meas Tech*, 4(7), 1445–1461, doi:10.5194/amt-4-1445-2011, 2011.
- 8 Siegenthaler, U., Friedli, H., Loetscher, H., Moor, E., Neftel, A., Oeschger, H. and B., S.:
9 Stable-isotope ratios and concentration of CO₂ in air from polar ice cores, *Ann. Glaciol.*,
10 10, 151–156, 1988.
- 11 Smith, H. J., Fischer, H., Wahlen, M., Mastroianni, D. and Deck, B.: Dual modes of the
12 carbon cycle since the Last Glacial Maximum, *Nature*, 400(6741), 248–250, 1999.
- 13 Steig, E. J., Ding, Q., White, J. W. C., Kuettel, M., Rupper, S. B., Neumann, T. A., Neff,
14 P. D., Gallant, A. J. E., Mayewski, P. A., Taylor, K. C., Hoffmann, G., Dixon, D. A.,
15 Schoenemann, S. W., Markle, B. R., Fudge, T. J., Schneider, D. P., Schauer, A. J., Teel,
16 R. P., Vaughn, B. H., Burgener, L., Williams, J. and Korotkikh, E.: Recent climate and
17 ice-sheet changes in West Antarctica compared with the past 2,000 years, *Nat. Geosci.*,
18 6(5), 372–375, doi:10.1038/NGEO1778, 2013.
- 19 Trudinger, C. M., Enting, I. G., Rayner, P. J. and Francey, R. J.: Kalman filter analysis of
20 ice core data - 2. Double deconvolution of CO₂ and delta C-13 measurements, *J.*
21 *Geophys. Res.-Atmospheres*, 107(D20), doi:10.1029/2001jd001112, 2002.
- 22 Welp, L. R., Keeling, R. F., Meijer, H. A. J., Bollenbacher, A. F., Piper, S. C.,
23 Yoshimura, K., Francey, R. J., Allison, C. E. and Wahlen, M.: Interannual variability in
24 the oxygen isotopes of atmospheric CO₂ driven by El Nino, *Nature*, 477(7366), 579–582,
25 2011.
- 26 Zhao, C. L., Tans, P. P. and Thoning, K. W.: A high precision manometric system for
27 absolute calibrations of CO₂ in dry air, *J. Geophys. Res. Atmospheres*, 102(D5), 5885–
28 5894, doi:10.1029/96jd03764, 1997.
- 29